The Path to Graphene Synthesis and Applications

Approved by:

Dr. W. J. Ready, Advisor
MSE, EOSL at GTRI
Georgia Institute of Technology

Dr. Brent Carter
MSE Undergraduate Coordinator
Georgia Institute of Technology

Dr. Zhitao Kang
College of Engineering
Georgia Institute of Technology

Date Approved: May 7, 2010

The Path to Graphene Synthesis and Applications

A Thesis
Presented to
Jeffrey A. Donnell
for LCC 4702

by

David A. Soracco

In Partial Fulfillment
of the Requirements for the
Undergraduate Research Opportunities Program in the
College of Engineering

Georgia Institute of Technology
May 2010

TABLE OF CONTENTS

LIST OF FIGURES

LIST OF TABLES

INTRODUCTION

Just as with carbon nanotubes before it, graphene is taking the research spotlight more and more often. An amazing material, graphene consists of one atomic layer of sp^2-hybridized carbon in a 2 dimensional lattice of hexagons. The stuff is incredibly versatile, exhibiting useful electrical, thermal, optical, quantum, mechanical and chemical properties. While initially fabricated using an extremely expensive and time consuming mechanical exfoliation technique, recent innovations have focused on production through epitaxial growth on SiC. Although scalable, the relatively high cost of SiC has prompted research into alternative methods. The growth of graphene over thin transition metal films (Ni, Cu) presents a viable, scalable process at a more manageable cost.

Moore's Law is a term coined decades ago to describe the logarithmic progression over the years of the number of transistors that can be fit on an integrated circuit. In the foreseeable future, current silicon-based electronics will reach a limit and the progression described by Moore's Law is predicted to end unless alternative technologies can be found. Graphene is on the vanguard of a new group of nanomaterials that can supply the electronics industry with the slew of novel properties needed to keep progress going at the steady pace illustrated by Moore's Law for so long. Cyclotron resonance has been used to determine speeds of around $1 \cdot 10^6$ m/s for electrons in graphene, which is the fastest velocity recorded for all known carbon materials [1]. Weak temperature dependence of electron transport in graphene allows for an intrinsic mobility of greater than 200,000$cm^2\ V^{-1}s^{-1}$, a much higher value than that of silver [2]. These impressive properties provide the motivation behind this research.

PRODUCTION

Many methods already exist to produce graphene, but they can vary greatly in terms of time spent, required facilities, and most importantly cost. While graphene that has been mechanically exfoliated from a 3D crystal of graphite can cost thousands of dollars for a tiny fragment (~\$1,000,000/cm^2 in April 2008), the same material epitaxially grown on SiC will cost the same as the substrate used to grow it (~\$100/cm^2) [3].

Since graphene is present in all 3D crystals of graphite, mechanical exfoliation was one of the earliest methods used to produce it. Researchers were initially only able to reliably produce crystals with hundreds of layers. It wasn't until Geim's group began to use plastic adhesive tape to pull apart multilayer fragments of graphite that monolayer graphene was confirmed as a freestanding material. In 2005, Geim's group found a more reliable way of producing the 2D crystals. "A fresh surface of a layered crystal was rubbed against another surface (virtually any solid surface is suitable), which left a variety of flakes attached to it (the rubbing process can be described as similar to 'drawing by chalk on a blackboard')" [4]. The method always produces a few monolayers among the many fragments and the desirable samples of graphene are identifiable by optical phase contrast microscopy. Selected crystals can be confirmed as graphene monolayers through analysis with an atomic force microscope (AFM). This method is useful for producing samples for laboratory analysis but cannot meet the needs of industrial-scale mass-production. Its greatest downside is the extensive time required to locate sought-after samples.

Currently, the most popular growth technique is implemented by heating SiC to temperatures of greater than 1100°C so that the carbon in the lattice can diffuse to the surface. The greatest drawback of this process is the relatively high cost of single crystal SiC substrates.

Properties of the resulting graphene are dependent on the face of the crystal used for growth. In any epitaxial growth process, the substrate used to grow graphene affects the material's properties if any bonding is present. The epitaxial growth of graphene on ruthenium produces excellent samples, but the initial layer interacts with the substrate to reduce the efficacy of graphene's electrical properties. "Whereas the first graphene layer couples strongly to the Ru substrate, the second layer is essentially decoupled and largely recovers the electronic structure of free-standing graphene" [5]. For this reason, two layers are desirable because the first one acts as a "buffer" layer. One of the advantages of graphene growth over a Ni film is that the Ni can be selectively etched away with dilute HCl or Fe_3Cl. The graphene film can then be easily cleaned and transferred to another substrate for anything from analysis to testing.

Kim *et al.* is one of a few groups who have recently synthesized graphene by chemical vapor deposition over a thin layer of nickel. A thin film of nickel catalyst is deposited by electron-beam evaporation onto a catalyst support layer, typically Si over SiO_2 but many substrates are suitable. The samples are then heated in a CVD furnace to 900-1000°C under an argon atmosphere. The key to the process is an annealing step that causes the Ni film to form grains. Hydrogen is flowed in during annealing to facilitate removal of impurities. After this step, a very dilute flow of CH_4 is broken down over the film and carbon is saturated into the Ni for a short time period. As the samples are subsequently cooled, the carbon diffuses to the surface of the grains and anywhere from 1-10 layers of graphene form. Kim's group "found that [a] fast cooling rate [of ~10°Cs^{-1}] is critical to suppressing formation of multiple layers and for separating graphene layers efficiently from the substrate in the later process" [6]. Another group determined that a slow cooling rate assured less diffusion of carbon to the grain boundaries, limited the formation of graphite at these particular nucleation sites [7]. This production method

is relatively easy to pursue in a laboratory setting. Graphene can be grown on thin nickel films and etched samples can be used for testing and device fabrication.

Material Properties and Applications

Although there are many diverse ways to produce pristine graphene, the material itself is still difficult to fabricate in large amounts and large sample sizes. It is important to understand the properties of this suddenly viable substance and while much is already known, five years is not enough time to have fleshed out all of graphene's properties. The following provides a brief review of recent discoveries with respect to the material's properties and possible applications.

Elasticity and Strength

The mechanical properties of graphene were examined by stretching them over a substrate that had large micron-sized holes. Even though they were tautly stretched, it was found that the graphene adheres to the vertical wall of each hole from 2 to 10 nm, likely due to van der Waals attraction. The mechanical properties of the free-standing graphene films were probed by indenting the center of each film with an AFM. Because of the strength of the films, cantilevers with diamond tips were used for this study. The data showed no hysteresis [from load cycling], which demonstrated the elastic behavior of the film and showed that the graphene film did not slip around the periphery of the well. The intrinsic strength is $\sigma^{2D}_{int} = 42 \pm 4$ N m^{-1}. This corresponds to Young's modulus of $E = 1.0 \pm 0.1$ TPa [8].

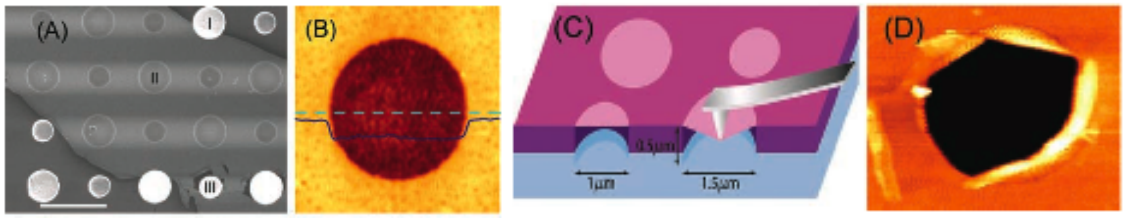

Figure 1. A shows an SEM micrograph of a large graphene flake suspended over an array of circular holes, scale bar 3 μm. B is a non-contact mode AFM image of graphene over one of the holes. The solid blue line is a height profile over the dashed line. The step height at the edge of the membrane is ~2.5 nm. C is a schematic of the nanoindentation process, and D is an AFM image of the fractured membrane III from A [7].

FRICTION AND DISSIPATION

While bulk graphite is a good lubricant, Filleter et al. has shown that single layer graphene (1LG) and bilayer graphene (2LG) outperform graphite. 1LG and 2LG are prepared for analysis *ex situ* on SiC(0001) using thermal decomposition to generate large graphene terraces. In order to be efficient, Filleter's group makes use of a homebuilt UHV-AFM system to accomplish three steps with one probe tip. They first identify the surface structure and layer thickness using Kelvin probe force microscopy in a noncontact AFM (nc-AFM) mode, then use friction force microscopy to conduct local friction measurements, and finally reimage the sample in nc-AFM mode to confirm a zero-wear regime. Measurements can be made in both modes with the same probe tip because cantilevers are used for both types of imaging.

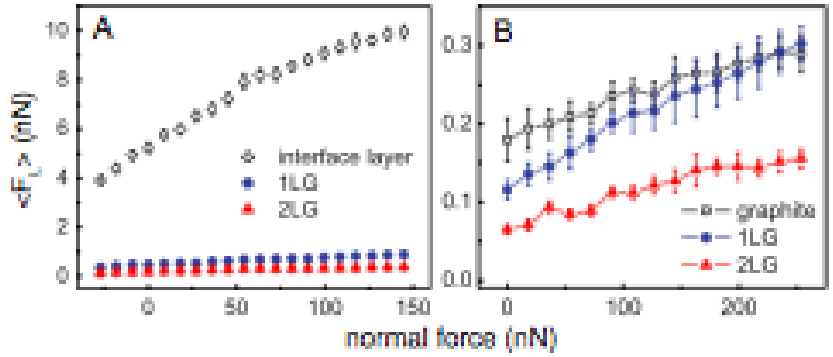

Figure 2. A is a plot of the average lateral force as a function of normal force. B is a plot of normal vs. average lateral force averaged over repeated measurements [9].

As the probe tip slides against the graphene, the lattice is locally distorted and released by the tip transferring kinetic energy into lattice vibrations. "In the case of the 1LG film, the associated lattice motion is damped by the creation of electronic excitations through *e*-ph coupling, much more so than in the case of 2LG films where the *e*-ph coupling is vanishingly small. For 2LG, undamped lattice vibrations excited during complex slip events reduce the average lateral force required for the tip to slide over the surface, similar to the way in which thermal vibrations reduce friction. For 1LG graphene however, lattice vibrations are more

efficiently damped, thereby removing this vibrational reduction of lateral force and dissipating more energy in the sample in the form of electron excitation" [10].

ELECTRICAL PROPERTIES

Graphene exhibits a nonuniversal minimum conductivity plateau in all experimental work thus far. One group examined this issue and produced a qualitative and semi-quantitative explanation. Their results provide a realistic mechanism for why disordered graphene (i.e. graphene that contains random charged impurities) has a minimum conductivity at low induced carrier densities. While their model does not describe in any way transport at the neutral-Dirac point, this transport theory is an "important step in the right direction" and "provides essential insights on how to obtain higher mobility, which is necessary if graphene is to have serious technological impact as an electronic material" [11].

Another group headed by Chen and Jang further explored the issue of graphene's unusual carrier-density-dependent conductivity. They probed the dependence of the conductivity of graphene on the density of charged-impurities by controlled potassium doping of clean crystals in ultra-high vacuum at low temperature. The results indicate "the minimum conductivity systematically depends on charged-impurity density, decreasing on initial doping, and reaching a minimum near $4e^2/h$ only for non-zero charged-impurity density, indicating that the universal conductivity at the Dirac point has not yet been probed experimentally" [12]. Another important finding is that the minimum conductivity point does not occur when the gate-induced carrier density neutralizes the impurity charge, but instead at the gate voltage at which the average impurity potential is zero.

SENSING

Graphene-based sensors have already received much acclaim in the scientific community. The material is sufficiently electronically quiet to allow for the detection of single molecules and

single electrons at room temperature, and it is very well suited for the ultrasensitive probing of magnetic fields or micromechanical strain. Schedin *et al.* find that equally as important is the prospect of "chemical doping of graphene by both electrons and holes in high concentrations without deterioration of its mobility" [13]. They see the microfabrication of p-n junctions on graphene as a worthwhile goal for the future.

THE FINE STRUCTURE CONSTANT

While it usually requires very sophisticated equipment and facilities to explore fundamental constants and their relation to materials properties, it is not common to find phenomena that are defined solely by fundamental constants.

> The opacity of suspended graphene is defined solely by the fine structure constant, $\alpha = e^2/\hbar c \approx 1/137$ (where c is the speed of light), the parameter that describes coupling between light and relativistic electrons and that is traditionally associated with quantum electrodynamics rather than materials science. Despite being only one atom thick, graphene is found to absorb a relatively significant ($\pi\alpha = 2.3\%$) fraction of incident white light, a consequence of graphene's unique electronic structure [14].

As a result, the value of the fine structure constant can be determined relatively easily, with simple equipment. This is useful because it provides another method of determining the number of layers produced. The percent of transmitted light decreases in multiples of 2.3, with each layer absorbing the same amount of light. This is possible due to the uniquely low reflectance (<0.1%) of pristine graphene [15].

This project aims to confirm growth of graphene samples over transition metal films by CVD through Raman spectroscopy and sheet resistance measurements. The parameters of the growth process will optimize the size of produced graphene samples by growth of larger Ni grains. In future work, graphene will be confirmed through analysis by AFM and TEM.

METHODS

Graphene was grown by chemical vapor deposition (CVD) in one of two furnaces, a FirstNano Thermal CVD quartz tube furnace and a Black Magic plasma enhanced (PECVD) furnace. All samples were prepared from one of two diced 4 in. n-type silicon wafers. Both wafers were oxidized in dry O_2 to produce 300 nm thick silica catalyst support layers. One oxidized wafer was coated with a 300 nm thick layer of Ni by electron-beam evaporation while the other was coated with 500 nm of Ni.

After an initial rinsing with acetone, methanol, and isopropanol with intermediate air drying steps, each sample was placed into one of the two furnaces and ramped up to a temperature ranging from 825-1000°C in an argon atmosphere. Once the furnaces reached peak temperature, the samples were soaked for a period ranging from 10-30 minutes in H_2 and Ar to remove impurities and anneal the sample to induce Ni grain growth. A dilute flow of CH_4 combined with H_2 and Ar was floated into the chamber for 5 min to grow the graphene film. A variation of the process used 1 min of growth time combined with a 5x larger methane flow rate. Subsequent cooling allowed removal of samples with multilayer graphene as a polycrystalline film conforming to the underlying Ni grains. Figure 3 below shows the process steps.

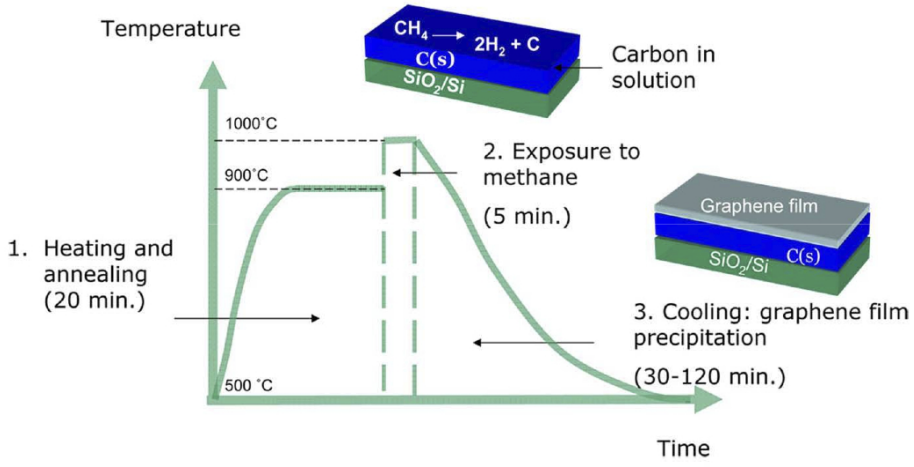

Figure 3. Process of Ni saturation and graphene growth upon cooling [7]

The parameters varied in each growth process were annealing temperature and duration, growth temperature and duration, methane flow rate, and the Ni catalyst layer thickness, and are shown in Tables 1 and 2 below. Samples were examined and imaged with an Olympus BH2 Optical Microscope at the 100 objective, or 1000x magnification. Those with confirmed grain growth were analyzed by Raman spectroscopy using a Renishaw InVia Raman Microscope at a wavelength of 532 nm to determine if graphene's characteristic 2D, and G peaks were present.

Table 1. Variables of runs performed on Black Magic PE-CVD

CH_4 flow rate [sccm]	**Anneal time [min]**	**Growth time [min]**	**Temperature [°C]**
20	15	5	825
70			
20	30		
70			

Table 2. Variables of runs performed on FirstNano Thermal CVD

CH_4 flow rate [sccm]	**Anneal time [min]**	**Growth time [min]**	**Temperature [°C]**
5	10	5	900
	30		
50	10	1	
	30		
5	10	5	1000
	30		
50	10	1	
	30		

The sheet resistances of samples were found using a Veeco FPP-100 Four Point Probe set to a thickness of 0.0432 cm, the thickness of each sample, and having a correction factor of 0.991. Backs of samples and silica surfaces were analyzed for comparison.

RESULTS

As shown in Figures 4 and 5, samples grown using the Black Magic PECVD showed extremely fine (<1 μm^2) grain growth when viewed under an optical microscope. This is likely due to the restriction of 825°C as a maximum temperature. The ratio of CH_4:H_2 was 20/70:1350, or 1.45/4.93vol% concentration.

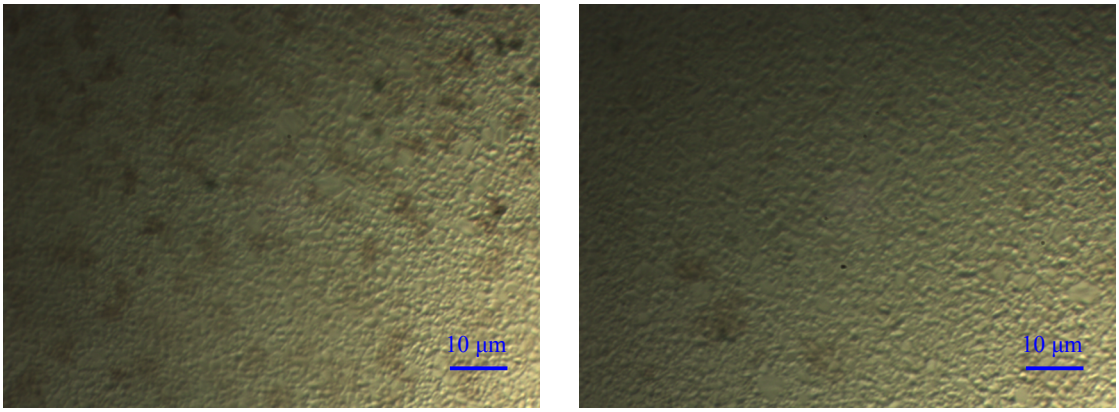

Figures 4 & 5. Optical images of fine Ni grains annealed for 15 and 30 min, respectively, at 825°C

Samples grown in the FirstNano Thermal CVD at a temperature exceeding 930°C left black spots on the film. As shown in Figures 5 and 6, larger grains (>20 μm^2) were achieved with longer annealing times. The ratio of CH_4:H_2 was 5/50:500, or 0.99/9.09vol% concentration.

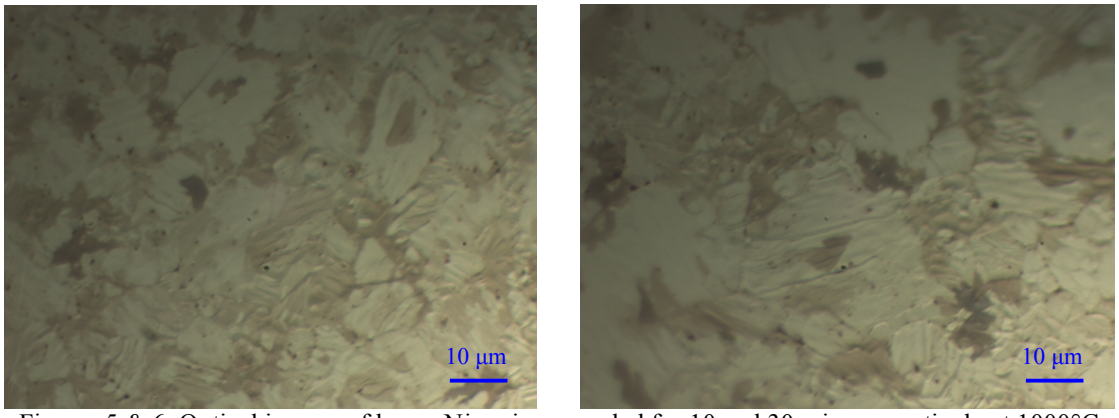

Figures 5 & 6. Optical images of larger Ni grains annealed for 10 and 30 min, respectively at 1000°C

The result of Raman characterization performed on one of these samples annealed for 10 min and grown at 1000°C is shown below in Figure 7. The sample was analyzed in a number of different grains. One light and dark region produced the desired Raman peaks.

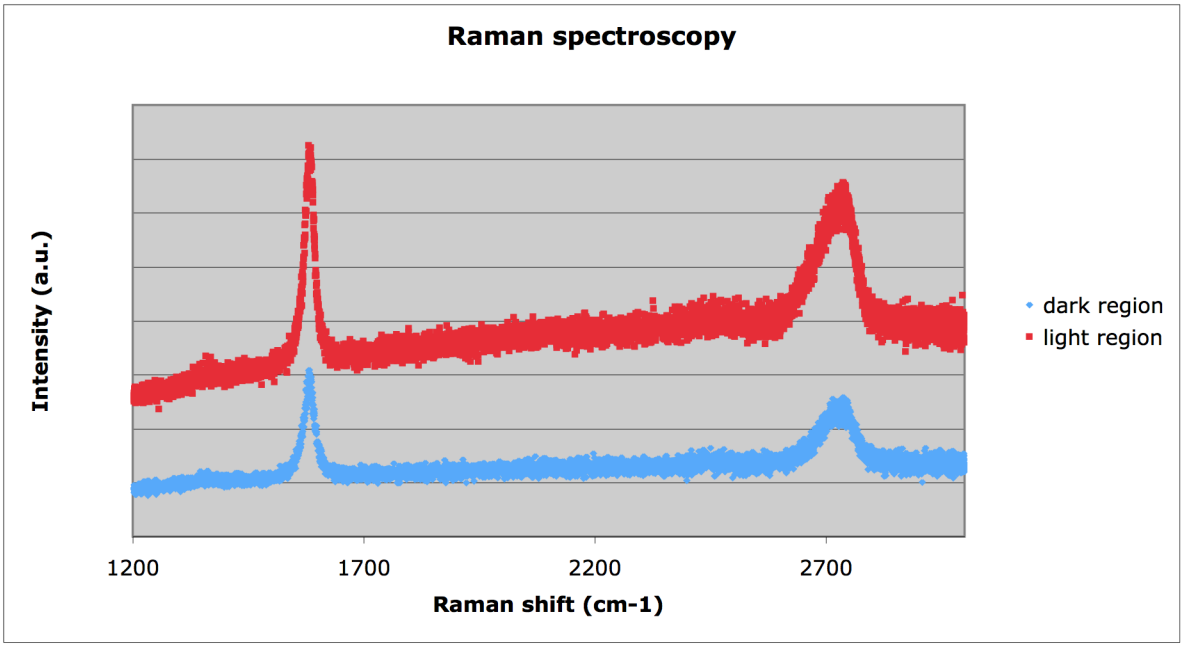

Figure 7. Raman characterization of a sample (shown in Figure 8) grown by thermal CVD over 500 nm Ni

An optical image of the locations where Raman characterization was performed is shown below in Figure 8. The light and dark regions closest to the center of the image are the locations where the 532 nm light source was focused.

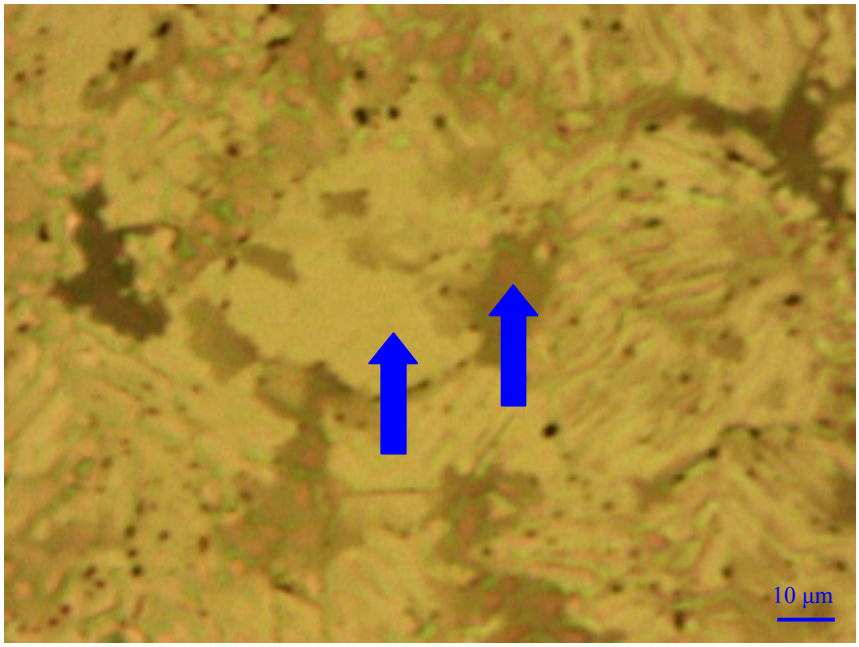

Figure 8. Optical image of light and dark regions used for Raman characterization

The four point probe used to conduct sheet resistance measurements had a probe spacing of 0.159 cm and correction factor (F) of 0.991. Samples were measured with a digital caliper and found to be 0.000445 m thick (t). A control sample with only deposited Ni and no growth or annealing was also analyzed for comparison. Measured resistances were converted to resistivities using the following equations:

$$R_s = R*F \qquad \rho = R_s*t$$

Table 3. Sheet resistance and resistivity calculations

CH_4 flow rate [sccm]	Anneal time [min]	Growth time [min]	Temperature [°C]	R_s [Ω/sq]		ρ [μΩm]	
				300nm Ni	500nm Ni	300nm Ni	500nm Ni
20	15	5	825	0.35	0.19	154.17	86.03
	30			0.19	0.35	86.03	157.26
70	15			0.44	0.24	197.78	104.84
	30			0.25	0.22	111.45	99.11
5	10		900	0.32	0.15	143.60	64.62
	30			0.35	0.11	155.94	47.44
50	10	1		0.28	0.07	123.34	30.83
	30			0.31	0.11	137.44	50.66
5	10	5	1000	0.55	0.34	243.60	151.97
	30			0.37	0.18	166.51	78.32
50	10	1		0.37	0.18	162.98	79.29
	30			0.35	0.15	155.94	67.97

Table 4. Sheet resistance and resistivity of control samples

	R_s [Ω/sq]		ρ [μΩ]	
	300nm Ni	500nm Ni	300nm Ni	500nm Ni
control	0.62	0.26	277	115
control backside	1.34	0.04	595	16.3

DISCUSSION

The graphite heating plates in the newly acquired Black Magic PECVD system require months of use before they can be pushed to higher temperatures than 825°C. This temperature wasn't high enough to induce significant grain growth. Any graphene monolayers that may have formed are too small for useful or easy analysis. Samples annealed and grown at higher temperatures in the FirstNano Thermal CVD did produce large grains with preferential sites for graphene nucleation.

Kim's group demonstrated that monolayers and few-layer films have peaks with smaller ratio's of I_G/I_{2D}. An example of their results is shown below in Figure 9.

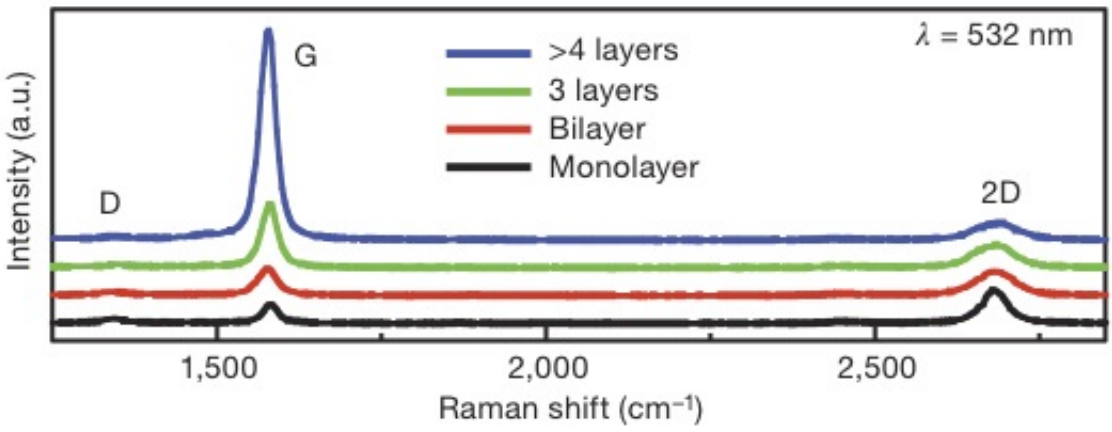

Figure 9. Raman characterization of 1 to few layers of graphene [6]

Although their work was conducted on exfoliated graphene, Ferrari *et al.* describes at length how Raman spectra can be used to determine a reasonable estimation of the number of graphene layers [16]. The G peak at 1580 cm^{-1} and the G' or 2D peak at 2700 cm^{-1} are the two most prominent features in the characterization. The G peak is caused by the doubly degenerate zone center E_{2g} mode, while the 2D peak is the second order of zone boundary phonons. These phonons also give rise to a small peak (D) at around 1350 cm^{-1} that is only present in defected graphene or graphite, and indicates the presence of a sample edge.

The greatest difference between bulk graphite samples and graphene is the ratio of G and 2D peak intensities. Graphite or many-layer graphene samples has a high I_G/I_{2D} and the 2D peak for graphite is split into two components, $2D_1$ and $2D_2$. These subpeaks are roughly ¼ and ½ the height of the G peak. Graphene samples produce a single sharp 2D peak that can be up to 4 times larger than the G peak. The ratio of G and 2D peaks in the Raman spectroscopy results indicate that many layers (3+) of graphene were analyzed. While the G peak is not significantly larger to indicate the presence of bulk graphite, this ratio is too large to be attributed to mono- or bilayer graphene.

The growth of too many graphene layers can be attributed to a too high vol% concentration of methane gas, as compared to work conducted by Reina *et al*. [7]. His group demonstrated that two types of samples were produced by their work, those with >0.7vol% methane concentrations and those with less than that critical amount. The more dilute flow resulted in high quantity (up to 87%) of bilayer and monolayer graphene, while higher concentrations of hydrocarbon gas resulted in very small number density of mono- and bilayer graphene with increased amount of multilayer graphene and graphitic formations at the grain boundaries. While it is possible that graphene was produced on the samples of this project, it is likely in small number density and a much more extensive Raman analysis is required to confirm this. Areas with much lower (<1) I_G/I_{2D} Raman results should be identified and further analyzed with AFM and then TEM analysis should be conducted if and when ratios of 0.3 to 0.5 are identified.

The sheet resistance measurements are quite high for a highly conductive material, but this could be due to high density of graphitic material formed at preferential nucleation sites in the grain boundaries of the Ni film. It is also possible that measurements could be affected by

coupling between graphene layers and the underlying nickel substrate due to the similarity in measurements between the control and the samples. These results further confirm a high probability of >3 graphene layers with extensive multilayer graphene growth. While all measured sheet resistances were comparable to each other, the extremely low resistivity of the control sample's backside might be an error due to a mistake or metal film contamination on the sample. While most resistivities were found to be lower than the control's, the two are close in value to each other and both higher than expected for Ni and graphene samples. This could be due to chemical doping or high impurity levels in the samples or a poorly calibrated four point probe.

The cooling rate of the Black Magic was considerably higher, peaking at 7°C/s while the highest cooling rate achieved by the FirstNano was slightly higher than 20°/min. Kim's group required a high cooling rate to ensure formation of fewer layers with higher hydrocarbon flow rates while Reina's group found that higher densities of mono- and bilayer regions were facilitated by a low hydrocarbon concentration and low cooling rate [6,7]. This work does not confirm or refute either group's assertion due to growth of too many layers, however their work shows that two different growth modes can be achieved to accommodate different equipment depending on hydrocarbon concentration and cooling rate.

CONCLUSIONS

While the goal of this research was to produce graphene samples by CVD over Ni films, Raman spectroscopy and sheet resistance measurements indicate that a large portion of the sample surface is covered with multilayer graphene or graphite as opposed to mono- or bilayer crystal. It cannot be concluded that the research was successful without further analysis by a more extensive Raman characterization and confirmation of results by AFM and ultimately

TEM. The effect of cooling rate cannot be commented on due to the similarity in resistance results obtained from samples grown using both furnaces.

FUTURE WORK

Future work will entail the optimization of the growth parameters to reliably produce large area fraction of mono- and bilayers of graphene. This will likely require greater dilution (<5 sccm) of the methane source gas and a better determination of the effects of cooling rate on the number of layers formed. Also, Cu can be substituted as the catalyst layer because recent work has shown that the copper can be evaporated from the substrate after and during growth [17]. This facilitates the film to be grown on the desired substrate without a necessary transfer step afterward. The only possible downside to the use of Cu over Ni is that the wrinkles that are induced into the film from the evaporation of the catalyst layer and resulting coefficient of thermal expansion mismatch might reduce the conductivity of grown samples.

Once a large enough sample is grown and transferred, light transmittance measurements can be conducted to confirm a correlation with the value of the fine structure constant with an optical microscope and opacity measurements. These measurements will also provide further confirmation of the number of layers present in each position of the sample.

With working samples of graphene films, Ni-made films can be transferred to other substrates by wet etching in dilute HCl and $FeCl_3$ [6] while Cu-made films can be used in their as-fabricated form for testing or device fabrication. Transferred samples can be suspended and attached to leads after cleaning of functional impurity groups from exposure in air to determine sensing properties. By far the most important aspect of the future work would be to produce larger area monolayer samples and find efficient ways maximize mono- and bilayer area coverage.

ACKNOWLEDGEMENTS

Many thanks to the help and use of equipment from members of GTRI's Nanolab at EOSL without whom this research couldn't have been possible: Dr. W. J. Ready, Stephan Turano, and Graham Sanborn. Thank you to Dr. Zhitao Kang for his comments and direction in reading and editing the thesis. Also, assistance with Raman characterization and equipment use was provided by Dr. Samuel Graham of the School of Mechanical Engineering at Georgia Tech. Sheet resistance measurements and use of a four point probe was provided by Mrs. Laureen Rose of the Microelectronic Research Center at Georgia Tech. And finally, thanks to Dr. Jeffrey Donnell for his patient tutelage and guidance in thesis writing.

REFERENCES

[1] K. Chuang, R.S. Deacon, R.J. Nicholas, K.S. Novoselov, and A.K. Geim, "Cyclotron resonance of electrons and holes in graphene monolayers," *Philosophical Transactions of The Royal Society A*, vol. 366, Jan. 2008, pp. 237-243.

[2] S.V. Morozov, K.S. Novoselov, M.I. Katsnelson, F. Schedin, D.C. Elias, J.A. Jaszczak, and A.K. Geim, "Giant Intrinsic Carrier Mobilities in Graphene and Its Bilayer," *Physical Review Letters*, vol. 100, Jan. 2008, pp. 016602-4.

[3] A.K. Geim and P. Kim, "Carbon Wonderland: Scientific American," *Scientific American Magazine*, Apr. 2008.

[4] K.S. Novoselov, D. Jiang, F. Schedin, T.J. Booth, V.V. Khotkevich, S.V. Morozov, and A.K. Geim, "Two-dimensional atomic crystals," *Proceedings of the National Academy of Sciences of the United States of America*, vol. 102, Jul. 2005, pp. 10451-10453.

[5] P.W. Sutter, J. Flege, and E.A. Sutter, "Epitaxial graphene on ruthenium," *Nature Materials*, vol. 7, May. 2008, pp. 406-411.

[6] K.S. Kim, Y. Zhao, H. Jang, S.Y. Lee, J.M. Kim, K.S. Kim, J. Ahn, P. Kim, J. Choi, and B.H. Hong, "Large-scale pattern growth of graphene films for stretchable transparent electrodes," *Nature*, vol. 457, Feb. 2009, pp. 706-710.

[7] Alfonso Reina, *et al.*, "Growth of large area single- and bi-layer graphene by controlled carbon precipitation on polycrystalline Ni surfaces," *Nano Research*, vol. 2, no. 6, June 2009, pp. 509-516.

[8] C. Lee, X. Wei, J.W. Kysar, and J. Hone, "Measurement of the elastic properties and intrinsic strength of monolayer graphene," *Science*, vol. 321, Jul. 2008, pp. 385-388.

[9] M. Ishigami, J.H. Chen, W.G. Cullen, M.S. Fuhrer, and E.D. Williams, "Atomic structure of graphene on SiO2," *Nano Letters*, vol. 7, Jun. 2007, pp. 1643-1648.

[10] T. Filleter, J.L. McChesney, A. Bostwick, E. Rotenberg, K.V. Emtsev, T. Seyller, K. Horn, and R. Bennewitz, "Friction and dissipation in epitaxial graphene films," *Physical Review Letters*, vol. 102, Feb. 2009, pp. 086102-4.

[11] S. Adam, E.H. Hwang, V.M. Galitski, and S. Das Sarma, "A self-consistent theory for graphene transport," *Proceedings of the National Academy of Sciences*, vol. 104, Nov. 2007, pp. 18392-18397.

[12] J. Chen, C. Jang, S. Adam, M.S. Fuhrer, E.D. Williams, and M. Ishigami, "Charged-impurity scattering in graphene," *Nat Phys*, vol. 4, May. 2008, pp. 377-381.

[13] F. Schedin, A.K. Geim, S.V. Morozov, E.W. Hill, P. Blake, M.I. Katsnelson, and K.S. Novoselov, "Detection of individual gas molecules adsorbed on graphene," *Nat Mater*, vol. 6, 2007, pp. 652-655.

[14] R.R. Nair, P. Blake, A.N. Grigorenko, K.S. Novoselov, T.J. Booth, T. Stauber, N.M.R. Peres, and A.K. Geim, "Fine structure constant defines visual transparency of graphene," *Science*, vol. 320, Jun. 2008, p. 1308.

[15] "Graphene Gazing Gives Glimpse Of Foundations Of Universe," *Science Daily*, Apr. 4, 2008. [Online]. Available: http://www.sciencedaily.com/releases/2008/04 /080403140918.htm [Accessed July 10, 2009].

[16] A. C. Ferrari, *et al.*, "Raman spectrum of graphene and graphene layers," *Physical Review Letters*, vol. 97, 187401 (2006).

[17] A. Ismach, *et al.*, "Direct chemical vapor deposition of graphene on dielectric surfaces," *Nano Letters*, doi: 10.1021/nl9037714, 2009.